Hole Transport Triphenylamine−Azomethine Conjugated System: Synthesis and Optical, Photoluminescence, and Electrochemical Properties

Danuta Sek,*,† Agnieszka Iwan,† Bozena Jarzabek,† Bozena Kaczmarczyk,† Janusz Kasperczyk,† Zbigniew Mazurak,† Marian Domanski,† Krzysztof Karon,‡ and Mieczyslaw Lapkowski†,‡

Centre of Polymer and Carbon Materials, Polish Academy of Science, 34 M. Sklodowska-Curie Str. 41-819 Zabrze, Poland, and Faculty of Chemistry, Silesian University of Technology, 44-120 Gliwice, M. Strzody 9, Poland

Received November 28, 2007; Revised Manuscript Received June 18, 2008

ABSTRACT: A series of six conjugated aromatic polyazomethines has been obtained by high-temperature solution polycondensation of diformyltriphenylamine with different primary aromatic diamines. The structures of polymers are characterized by means FTIR, ^{1}H NMR, and ^{13}C NMR spectroscopy and elemental analysis; the results show an agreement with the proposed structure. Polyazomethines emitted blue or blue-green light. Relative PL intensity of the polymers investigated in chloroform solution was found about 0.30%, while for doped ones it was about 20% in relation to 9,10-diphenylanthracene. Additionally, the photoluminescence spectra of the polyazomethines in polymer blend with poly(methyl methacrylate) (PMMA) have also been described. The lowest optical band gap value at 2.41 eV was detected. Polymers were investigated also by cyclic voltametry and differential pulse voltammetry in dichloromethane. An influence of different types of dopants, i.e., methanesulfonic acid (MSA), camphorsulfonic acid (CSA), *m*-cresol (MC), *p*-chlorophenol (PC), and *p*-pentadecylphenol (PDP), on absorption and emission wavelengths was investigated.

1. Introduction

Recently, organic hole-transporting materials are intensively researched as thin-layer electro-optical devices including organic light-emitting diodes (OLEDs), solar cells (SCs), organic field-effect transistors (OFETs), and photorefractive holographic materials (PRHMs).[1] Among them, much attention is paid to triphenylamine (TPA) derivatives because they are promising candidates for photoluminescence and electroluminescence materials.[2−15] TPA is a unique molecule possessing useful functions such as redox activity, fluorescence, ferromagnetism due to the high oxidizability of the nitrogen center, and transportability of positive charge centers via the radical cation species.[16] TPA possess a wide range of applications due to their outstanding physical, photochemical, and electrochemical properties. Being efficient hole conductors, triarylamines are commonly used as photoconductors in the Xerox process in laser printers and photocopiers.[17−19] Introduction of vinyl, acetylene, or azomethine moieties in TPA may lead to new functional materials based on the synergistic effect of both of them.[3−6] Most light-emitting polymers consist of aryl or heterocyclic structures often with various substituents, linked with vinyl and acetylene units.[2] Relatively less attention was paid to polymers with imine groups (−C═N−), i.e. polyazomethines and polyketanils. However, polyazomethines containing the nitrogen atom in the main chain with hybridization sp^2 has attracted a deal of interest due to the potential application of such compounds in electronics, optoelectronics, and photonics.[20−26] A further approach to obtain new polyazomethines is the introduction of bulky triarylamine into the molecules due to their less trend of aggregation.[27−29] This can reduce the crystallization propensity and improve the hole-transporting ability of the materials. It is well-known that triarylamine derivatives are used to fabricate multilayer organic layer emitting diodes (OLEDs) due to their carrier mobility and balance of the carriers populations in OLEDs. Few polymers exhibiting triphenylamine and imine structures in the main chains were synthesized from triphenylamine functionalized with amine groups.[10,11] Niu et al.[10,11] obtained polyazomethines in the reaction of 4,4′-diaminotriphenylamine and terephthalic aldehyde and glyoxal and studied them as hole transporting materials. The authors found that blue photoluminescence exhibited only the polymer synthesized from terephthalic aldehyde. Polymer bearing glyoxal units, mainly due to the twisting conformations, could not be used as a blue-emitting layer as well as a hole transporting layer. Also, poly(*p*-phenylenevinylene)s (PPVs) containing triphenylamine unit are intensely studied.[12−15] The group of Tian[12−14] and He et al.[15] synthesized polymers containing a triphenylamine unit and vinylene or cyanovinylene linkages in the polymer chains, which emitted yellowish-green light.

On the other hand, the use of noncovalent interactions between molecules possessing the desired complementary structural elements is a crucial synthetic tool due to its great potential in the design of new, highly functional materials. The self-assembly processes of organic systems driven by protonation may be used to obtain structural variation and specifically physical properties for potential applications of these materials. Protonation is one of the important noncovalent interactions playing a fundamental role in polymer properties as well as in the design of new polymer architectures.[30] Polyazomethines are an interesting group of conjugated polymers having carbon−nitrogen double-bonded units in the main chain, capable of protonation and complexation. Polyazomethines in the most cases are insoluble in common solvents, and complexation of imine groups improves solubility what was reported by Jenekhe et al.[31] He also observed bathochromic shift of electronic absorption spectra after complexation polyazomethines with $GaCl_3$ and diphenyl- or di-*m*-cresyl phosphate. The reverse behavior was found by Cho et al.[32] Fluorene-based polyazomethines after complexation with sulfonated polystyrene exhibited hypsochromic shift of UV−vis spectra in comparison to the

* Corresponding author. E-mail: danuta.sek@cmpw-pan.edu.pl.
† Polish Academy of Science.
‡ Silesian University of Technology.

10.1021/ma702637k CCC: $40.75
Published on Web 08/26/2008

pristine ones. But it is interesting that those polymers after complexation gave a high luminescence in the solution although the pristine polymer did not show luminescence in a solution and film. None or very low intensity of polyazomethines luminescence was also reported in ref 33. However, polyazomethines with some another fluorophore structure in the polymer chains can exhibit high intensity of luminescence as it was described in ref 34. The authors[34] found that changing aprotic solvent (NMP) over formic acid caused hypsochromic shift of emission wavelength along with decrease of luminescence intensity.

Inspired by the above-described findings, we have undertaken a detailed study of the structure−spectroscopic properties in a series of new polyazomethines (abbreviated hereinafter as Ps) synthesized from 4,4′-diformyltriphenylamine and various primary aromatic diamines for the field of optoelectronics. Apart from this molecular engineering, the polyazomethines properties were also tuned by supramolecular engineering via protonation and H-bond formation with proper dopants: methanesulfonic acid (MSA), camphorsulfonic acid (CSA), *m*-cresol (MC), *p*-chlorophenol (PC), and *p*-pentadecylphenol (PDP).

2. Experimental Section

2.1. Materials. 1,4-Phenylenediamine (Aldrich), 4,4′-diaminobiphenyl (benzidine) (Fluka AG), 2,3,5,6-tetramethyl-1,4-phenylenediamine (Aldrich), 3,3′,5,5′-tetramethylbenzidine (Aldrich), *o*-tolidine (3,3′-dimethylbenzidine, 4,4′-bianisidine) (Aldrich), *o*-dianisidine (3,3′-dimethoxybenzidine, Fast Blue B) (Aldrich), triphenylamine (Aldrich), methanesulfonic acid (MSA) (Fluka AG), 4-chlorophenol (PC) (Aldrich), 3-pentadecylphenol (PDP) (Aldrich), camphorsulfonic acid (CSA) (Aldrich), hexamethylphosphoramide (HMPA) (Aldrich), and *N,N*-dimethylformamide (DMF) were used as received. *m*-Cresol was distilled before used. 4,4′-Diformyltriphenylamine (4,4′-(phenylimino)bisbenzaldehyde) was prepared by the Vilsmeier reaction according to the method described in the literature.[35] The solid was purified by column chromatography on silica gel (60 μm) using ethyl acetate/hexane (3:1) as the eluent to obtain 4,4′-diformyltriphenylamine as a main product (yield 77%, mp 146 °C). FTIR spectrum (KBr pellet): 3065, 2803, 2734, 1693, 1586, 1566, 1505, 1494, 1457, 1426, 1391, 1332, 1293, 1274, 1217, 1167, 1111, 955, 903, 831, 762, 724, 719, 702, 646, 628, 533, 518. ^{1}H NMR (600 MHz, $CDCl_3$, ppm): δ = 9.88 (s, 2H); 7.76−7.80 (m); 7.40 (t, 2H); 7.27 (t, 1H); 7.19 (m, 6H). ^{13}C NMR (150 MHz, $CDCl_3$, ppm): δ = 122.68; 126.99; 130.08; 131.23; 145.42; 151.93; 190.43 (HC═O). Anal. Calcd for $C_{20}H_{15}NO_2$ (301.339): C, 79.73; H, 4.98; N, 4.65. Found: C, 79.44; H, 5.07; N, 4.67. Side products were the following. 4-Monoformyltriphenylamine (yield 12%, mp 124 °C). ^{1}H NMR (600 MHz, $CDCl_3$, ppm): δ = 9.81 (s, 1H); 7.66−7.69 (m, 2H); 7.00 (d, 2H)); 7.15−7.34 (m)). 4,4′,4″-Triformyltriphenylamine (yield 1%, mp 235 °C): ^{1}H NMR (600 MHz, $CDCl_3$, ppm): δ = 9.95 (s, 3H); 7.83−7.87 (d, 6H); 7.23−7.27 (m) (see Figure 1a).

2.2. Characterization Techniques. Analytical thin-layer chromatography (TLC) was performed on silica gel plates from E. Merck (silica gel F_{254}). Silica gel column chromatography was carried out with silica gel 60 from Merck (silica gel 60, spherical 40−50 μm). The obtained compounds were characterized by the following techniques: elemental analysis (240C Perkin-Elmer analyzer), ^{1}H NMR (Varian Inova 600 spectrometer, $CDCl_3$ solvent against TMS as an internal reference), and FTIR. Infrared spectra were acquired on a DIGILAB FTS-40A Fourier transform infrared spectrometer in the range of 4000−400 cm^{-1} at a resolution of 2 cm^{-1} and for an accumulated 32 scans. Samples were analyzed in a form of solutions in chloroform, films after evaporating $CHCl_3$ onto potassium bromide plates, and as pellets in potassium bromide. Melting point and T_g of the synthesized compounds were determined by differential scanning calorimetry (DSC) on a TA-DSC 2010 apparatus using sealed aluminum pans under a nitrogen atmosphere. UV−vis absorption spectra were recorded using a Hewlett-Packard 8452A spectrophotometer whereas the photoluminescence solution spectra were registered on a Fluorolog 3.12 Spex spectrometer with a 400 nm excitation line (450 W xenon lamp as the light source). For electrochemical measurements a CH Instruments 620A potentiostat was used. The cyclic voltammetry (CV) and differential pulse voltammetry (DPV) experiments were carried out in a three-electrode electrochemical cell. A platinum disk (diameter 1.0 mm) and platinum wire were used as working and counter electrodes, respectively, and an Ag/Ag^+ electrode as a reference. In all experiments the sample concentration was 0.5 mmol/L, and a 0.2 M solution of Bu_4NPF_6 (Aldrich 98% purity) in dry dichloromethane was used as a supporting electrolyte solution. Cyclic voltammetry measurements were performed at a scan rate of 100 mV/s at room temperature. All solutions have been deaerated with Ar gas prior to the experiments. Current−voltage measurements were performed on an ITO/polymer/Alq_3/Al device. The polyazomethine solution (1% w/v in chloroform) was spun-cast onto an ITO-covered glass substrate at room temperature. Residual solvent was removed by heating the film (thickness about 200 nm) in a vacuum. The Alq_3 layer was prepared on the polymer film surface by vacuum deposition at a pressure of 2×10^{-4} Pa, and then the Al electrode was vacuum-deposited at the same pressure. The area of the diodes was 9 mm^2. Current−voltage characteristics were detected using a Keithey 6715 electrometer.

2.3. Synthesis of Polymers. A detailed procedure is the following: 0.075 g (0.25 mmol) of 4,4′-diformyltriphenylamine, 0.25 mmol of diamine, 0.004 g of *p*-toluenesulfonic acid (PTS), and 5 mL of hexamethylphosphoramide (HMPA) were introduced into a 20 mL, two-necked, round-bottomed flask equipped with an overhead stirrer, a reflux condenser, and an argon inlet. The mixture was stirred and heated at 160 °C for 6 h in an oil bath. After cooling, the solution was poured into 50 mL of methanol. The polymer was precipitated, then filtered and washed with hot methanol (Soxhlet apparatus), and finally dried at 50 °C under reduced pressure.

Synthesis of P1. Yield: 0.08 g, 85%. FTIR spectrum (KBr pellet): 3059 and 3027 (ν CH), 1694 (ν C═O), 1618 (ν C═N), 1591, 1506, 1490, 1455, 1428, and 1417 (ν Ph), 1318 (δ CH), 1284 (ω CH), 1260 sh (δ CH/ν Ph−N), 1195 (ν Ph−N═), 1168 and 1105 (δ CH), 975, 879, and 835 (γ CH), 754 and 696 (γ Ph). ^{1}H NMR (600 MHz, $CDCl_3$, ppm): δ = 8.46 (s, H-1); 7.81 (d, H-2); 7.15−7.21 (m, H-3, H-5, H-7); 7.36 (dd, H-6); 7.27 (s, H-4), code as in Figure 3. ^{13}C NMR (150 MHz, $CDCl_3$, ppm): δ = 158.57 (HC═N), 152.61, 149.95, 146.39, 131.28, 129.97, 129.72, 126.65, 123.29, 121.80, 115.59. UV−vis recorded in chloroform λ_{max} at 419 nm. Anal. Calcd for $C_{26}H_{20}N_3$ (374.465): C, 83.65; H, 5.09; N, 11.26. Found: C, 82.18; H, 5.12; N, 11.10. T_g, DSC: 195 °C.

Synthesis of P2. Yield: 0.10 g, 82%. FTIR spectrum (KBr pellet): 3060 and 3026 (ν CH), 1693 (ν C═O), 1621 (ν C═N), 1586, 1504, 1486, 1455, 1428, and 1417 (ν Ph), 1318 (δ CH), 1284 (ω CH), 1260 sh (δ CH/ν Ph−N), 1196 (ν Ph−N═), 1166 and 1109 (δ CH), 975, 883, and 828 (γ CH), 757 and 696 (γ Ph). ^{1}H NMR (600 MHz, $CDCl_3$, ppm): δ = 8.47 (s, H-1); 7.83 (d, H-2); 7.15−7.21 (m, H-3, H-5, H-7); 7.38 (dd, H-6); 7.31 (d, H-8); 7.66 (d, H-9), code as in Figure 3. ^{13}C NMR (150 MHz, $CDCl_3$, ppm): δ = 159.08 (HC═N), 151.22, 149.90, 146.36, 138.11, 131.29, 130.05, 129.74, 127.57, 126.13, 123.30, 121.44, 115.39. UV−vis recorded in chloroform λ_{max} at 417 nm. Anal. Calcd for $C_{32}H_{24}N_3$ (450.561): C, 85.53; H, 5.12; N, 9.35. Found: C, 83.12; H, 5.32; N, 9.46. T_g, DSC: 275 °C.

Synthesis of P3. Yield: 0.08 g, 70%. FTIR spectrum (KBr pellet): 3059 and 3031 (ν CH), 2988, 2918, and 2865 (ν CH_3), 1695 (ν C═O), 1631 (ν C═N), 1592, 1505, 1491, 1457, and 1419 (ν Ph), 1380 (δ CH_3), 1318 (δ CH), 1284 (ω CH), 1260 sh (δ CH/ν Ph−N), 1216 (δ CH/ν Ph−N), 1168, 1107, and 1062 (δ CH), 953, 878, and 830 (γ CH), 757 and 696 (γ Ph). ^{1}H NMR (600 MHz, $CDCl_3$, ppm): δ = 8.12 (s, H-1); 7.84 (d, H-2); 7.16−7.26 (m, H-3, H-5, H-7); 7.38 (dd, H-6); 2.12 (s, CH_3), code as in Figure 3. ^{13}C NMR (150 MHz, $CDCl_3$, ppm): δ = 161.92 (HC═N), 152.70, 149.87, 147.76, 131.28, 129.69, 129.59, 126.64, 124.79, 123.67, 120.96, 15.01 (CH_3). UV−vis recorded in chloroform λ_{max} at 337 and 387

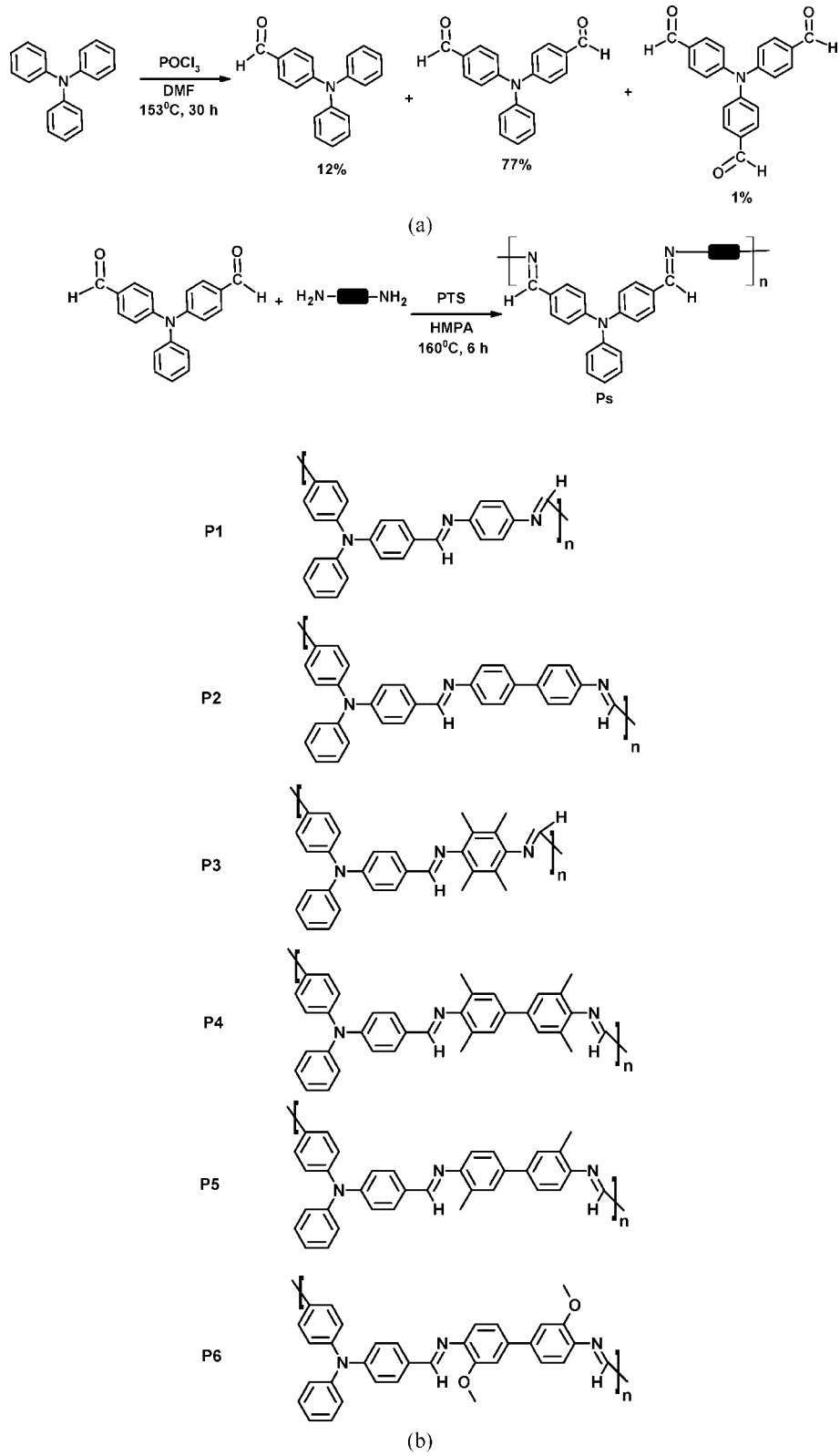

Figure 1. Synthetic route of the aldehyde (a) and synthetic route and chemical structure of the synthesized polyazomethines (b).

nm. Anal. Calcd for $C_{30}H_{28}N_3$ (430.571): C, 83.91; H, 6.29; N, 9.79. Found: C, 82.79; H, 6.34; N, 9.71. T_g, DSC: 214 °C.

Synthesis of P4. Yield: 0.10 g, 75%. FTIR spectrum (KBr pellet): 3058 and 3027 (ν CH), 2966, 2943, 2912, and 2865 (ν CH_3), 1695 (ν C═O), 1631 (ν C═N), 1592, 1505, 1491, and 1430 (ν Ph), 1470 and 1376 (δ CH_3), 1318 (δ CH), 1284 (ω CH), 1260 sh (δ CH/ν Ph−N), 1187, 1167, 1107, and 1090 (δ CH), 1062, 983, and 854 (γ CH), 757 and 696 (γ Ph). ^{1}H NMR (600 MHz, $CDCl_3$, ppm): δ = 8.20 (s, H-1); 7.83 (d, H-2); 7.15−7.24 (m, H-3, H-5, H-7); 7.37 (dd, H-6); 7.32 (s, H-8); 2.23 (s, CH_3), code as in Figure 3. ^{13}C NMR (150 MHz, $CDCl_3$, ppm): δ = 161.05 (HC═N), 150.32, 150.05, 146.52, 136.40, 131.32, 129.81, 129.71, 127.64, 126.77, 126.52, 123.32, 121.97, 18.54 (CH_3). UV−vis recorded in chloroform λ_{max} at 340 and 390 nm. Anal. Calcd for $C_{36}H_{32}N_3$ (506.667): C, 85.54; H, 6.14; N, 8.32. Found: C, 83.78; H, 6.26; N, 8.30. T_g, DSC: 230 °C.

Synthesis of P5. Yield: 0.11 g, 85%. FTIR spectrum (KBr pellet): 3061 and 3026 (ν CH), 2946, 2917, 2870, and 2852 (ν CH_3), 1696

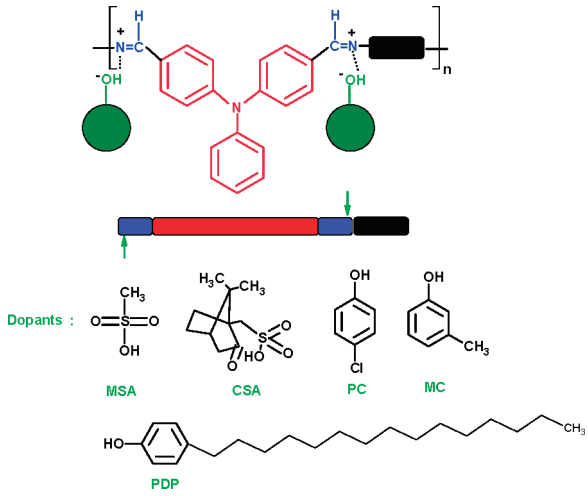

Figure 2. Proposed schematic model for the interaction between the polyazomethines chains and protonating agent.

(ν C=O), 1623 (ν C=N), 1589, 1505, 1489, 1453, 1428, and 1417 (ν Ph), 1481 and 1376 (δ CH_3), 1318 (δ CH), 1284 (ω CH), 1260 sh (δ CH/ν Ph−N), 1206 (ν Ph−N=), 1168, 1124, and 1060 (δ CH), 975, 879, 831, and 812 (γ CH), 754 and 696 (γ Ph). ^{1}H NMR (600 MHz, $CDCl_3$, ppm): δ = 8.36 (s, H-1); 7.84 (d, H-2); 7.15−7.21 (m, H-3, H-5, H-7); 7.37 (dd, H-6); 7.49 (s, H-8); 7.46 (d, H8′), 7.01 (d, H-9), 2.44 (s, CH_3), code as in Figure 3. ^{13}C NMR (150 MHz, $CDCl_3$, ppm): δ = 158.12 (HC=N), 150.26, 149.84, 146.53, 138.10, 132.50, 131.22, 129.97, 129.75, 128.78, 126.10, 125.13, 124.74, 123.35, 118.03, 18.12 (CH_3). UV−vis recorded in chloroform λ_{max} at 412 nm. Anal. Calcd for $C_{34}H_{28}N_3$ (478.614): C, 85.53; H, 5.67; N, 8.80. Found: C, 84.04; H, 5.74; N, 8.57. T_g, DSC: not detected to 300 °C.

Synthesis of P6. Yield: 0.08 g, 63%. FTIR spectrum (KBr pellet): 3060 and 3033 (ν CH), 2998, 2933, 2870, and 2832 (ν CH_3), 1691 (ν C=O), 1623 (ν C=N), 1588, 1559, 1505, 1489, 1463, 1428, and 1417 (ν Ph), 1481 and 1393 (δ CH_3), 1318 (δ CH), 1285 (ω CH), 1260 sh (δ CH/ν Ph−N), 1243, 1195 (ν Ph−N=), 1168 (δ CH), 1129 (δ CH/ν CO), 1029 (ν CO/ρ'CH_3), 875, 880, 831 (γ CH), 754 and 696 (γ Ph). ^{1}H NMR (600 MHz, $CDCl_3$, ppm): δ = 8.47 (s, H-1); 7.85 (d, H-2); 7.15−7.21 (m, H-3, H-5, H-7); 7.36 (dd, H-6); 7.22 (s, H-8); 7.18 (d, H8′), 7.09 (d, H-9), 3.95 (s, OCH_3), code as in Figure 3. ^{13}C NMR (150 MHz, $CDCl_3$, ppm): δ = 160.15 (HC=N), 152.64, 149.92, 146.44, 141.31, 139.44, 131.27, 130.17, 129.69, 126.60, 124.75, 123.29, 120.56, 119.68, 110.42, 56.10 (OCH_3). UV−vis recorded in chloroform λ_{max} at 413 nm. Anal. Calcd for $C_{34}H_{28}N_3O_2$ (510.613): C, 80.16; H, 5.30; N, 8.25. Found: C, 79.11; H, 5.40; N, 8.19. T_g, DSC: 178 °C.

2.4. Protonation of Polymers. Protonation of the polyazomethines with MSA, MC, PC, and PDP was carried out at room temperature in chloroform solution (concentration 10^{-4} mol/L). The mole ratio of the dopant to the polymer mer unit was 2:1.

2.5. Preparation of Polymer Blends. Blends were obtained by dissolving the polyazomethine and nonemissive polymer poly(methyl methacrylate) (PMMA) in chloroform to form a homogeneous solution (concentration 0.1%). Films cast on glass were dried in a vacuum oven at 100 °C over 24 h.

3. Results and Discussion

Polyazomethines can be prepared from dialdehyde and diamines via high-temperature solution polycondensation in hexamethylphosphoramide (HMPA), as depicted in Figure 1b.

In our case 4,4′-diformyltriphenylamine was chosen as chromofore unit, which not only has a hole transporting property but can also reduce the rigid-rod conformation, thus improving the processability of the material. The yield of the polymers was in the range of 63−85% (see Experimental Section). All the polymers formed transparent films with good optical quality. Structures of the polyazomethines were confirmed by elemental analysis as well as FTIR, ^{1}H NMR, and ^{13}C NMR spectroscopy. Elemental analyses show good agreement of the calculated and found content of nitrogen and hydrogen in the polymers when repeated units structures were taken into calculations (see Experimental Section). However, a deficiency of carbon content of 1.0−2.4% was observed, and this is likely a result of difficulties in burning these polymers. Similar results were described for other Schiff's bases.[31]

As a lone electron pair in the nitrogen atom of the imine group can be protonated or can form an H-bond with a proper agent, the polyazomethines were also tested after doping (see Figure 2).

3.1. NMR of the Polyazomethines. Before investigation of NMR spectra of the polyazomethines, ^{1}H NMR spectra of 4-monoformyltriphenylamine, 4,4′-diformyltriphenylamine, and 4,4′,4″-triformyltriphenylamine obtained by the Vilsmeier reaction (see Figure 1a) were analyzed (see Experimental Section). In particular, the signals in the range of 9.81−9.95 ppm, present in the spectra of aldehydes, confirm the existence of the aldehyde group proton atoms. Thus, the presence of an one carbonyl group (in 4-monoformyltriphenylamine) results in a downfield shift of the line related to the carbonyl group in 4,4′-diformyltriphenylamine. On the other hand, the three carbonyl groups (in 4,4′,4″-triformyltriphenylamine) induce an upfield shift of the signal related to the carbonyl proton atom in 4,4′-diformyltriphenylamine (see Experimental Section). In the goal to obtain new polyazomethines, the aldehyde pure fraction of 4,4′-diformyltriphenylamine (purified by column chromatography) was used.

Polyazomethines expected chemical constitution is clearly confirmed by spectroscopic studies. In the Experimental Section NMR data concerning all polymers investigated are collected. In particular, the signals in the range of 158−162 ppm, present in the ^{13}C NMR spectra of all polymers, confirm the existence of the azomethine group carbon atoms. The changes in the chemical shift, observed upon the modification of the chemical constitution of the diamine originating subunit of the repeat unit, are cleary observed. For example, in the case of P3 and P4, the presence of four methyl groups in the ortho position with respect to nitrogen results in an upfield shift of the line related to the azomethine carbon atom in comparison with P1 and P2, respectively. Similar behavior for P6 was observed. On the other hand, the presence of two methyl groups in the ortho position with respect to nitrogen (P5) induces a downfield shift of the line related to the azomethine carbon atom in comparison with P2 and P4.

Most signals were assigned based on well-known proton NMR chemical shift displacements resulting from electron shielding/deshielding of the hydrogen nuclei by the inductive effects or from the diamagnetic anisotropy of various neighboring groups. In the Experimental Section ^{1}H NMR data concerning all polymers investigated are collected together with the assignment of the registered NMR lines. ^{1}H NMR spectra of the polymers are present in Figure 3.

For example, the inductive effect of the electron-rich ether linkage of the *o*-dianisidine segment (P6) has a deshielding effect on the phenyl rings ortho-oxygen protons, thus their shifts to higher frequency (H-8; 7.49 ppm). The induced magnetic field resulting from circulating π-electrons found in the methyl groups has a shielding effect on the azomethine bond and consequently shifting them to lower frequency. For example, in the polymers P1 and P2 the signal from the imine group at 8.46 ppm was observed, while the presence of the methyl substituents in aromatic rings in P3 and P4 caused significant upfield shift of the imine proton signals to 8.12 and 8.20 ppm, respectively. In the case of P6, the presence of the methoxy groups in the ortho

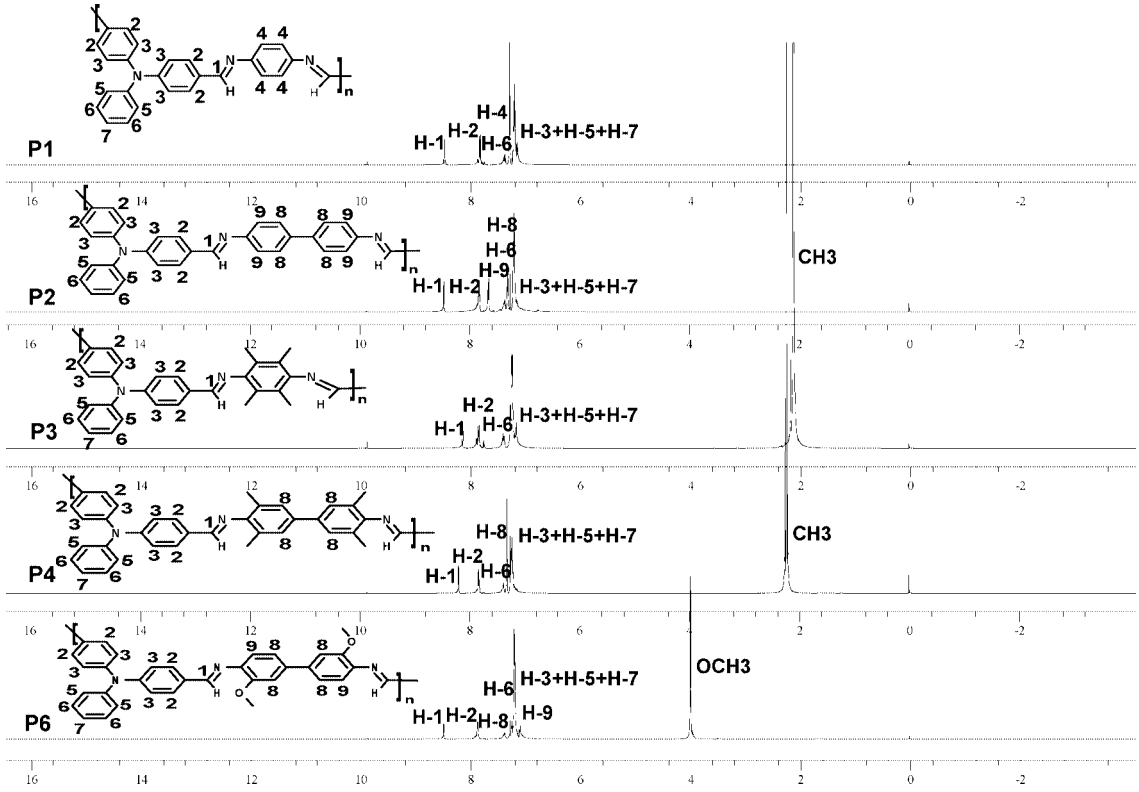

Figure 3. [1]H NMR spectra of the polyazomethines.

position with respect to nitrogen results in a upfield shift of the line related to imine proton in comparison with P2 and P5 (see Experimental Section). The upfield shift of the imine signals indicates less conjugation of the polymer chain.

No chemical shift of the imine group proton was observed after protonation with MSA and in the presence of phenol dopants.

3.2. FTIR Investigations. The presence of the imine groups is also confirmed by FTIR spectroscopy since in each case the band characteristic of the −HC═N− stretching deformations is detected. The exact position of this band varies in the spectral range 1618−1634 cm^{-1}, shifting toward higher wavenumbers for the polymers with the four methyl groups in the subunits. Assignments of particular bands appearing in FTIR spectra of the polyazomethines investigated are shown in the Experimental Section. In addition to the HC═N stretching band, a band at about 1590 cm^{-1} can be distinguished and ascribed to the C═C stretching deformations in the aromatic ring. Absorption at shorter wavelength being in the range of 1618−1623 cm^{-1} was observed for the polyazomethines P1, P2, P5, and P6 (see Experimental Section). The position of the azometine band is shifting toward higher wavenumbers for the polymers P3 and P4 and shows an intense absorption band at 1631 and 1634 cm^{-1}, respectively. The higher wavenumber value indicates that the bond between carbon and nitrogen atoms in the imine group is shorter, which means that the π-electrons in the double bond are less involved in conjugation. Theoretical calculation for the isolate azomethine (HC═N−) group, without substituents, gives the absorption band value at 1660 cm^{-1}. The lower wavenumber of the imine group absorption indicates the better conjugation of π-electrons caused by influence of adjusted group to the azomethine linkage.

Protonation of the polyazomethines with MSA in the molar ratio of SO_3H to −HC═N− group 1:1 causes a slight changes at the positions and at the intensities of bands in FTIR spectra of investigated compounds. Typical FTIR spectra of the polyazomethines P2, P4, and P5 before and after protonation with MSA are presented on Figure 4.

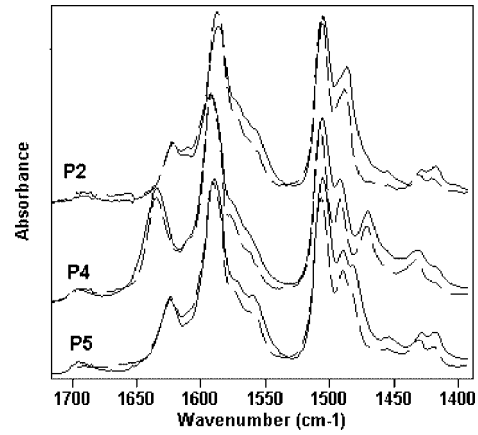

Figure 4. FTIR spectra of the unprotonated (solid line) and MSA protonated polyazomethines P2, P4, and P5 (dotted line).

3.3. Glass Transition Temperature. All synthesized polymers give similar DSC profiles with no melting endotherms and a clear T_g. These findings clearly indicate their amorphous nature. The DSC curves recorded with repeated heating−cooling cycles allowed the evaluation of T_g values of the synthesized polyazomethines in the range of 178−275 °C (see Experimental Section). It is obvious that they depend on the structure of the polymers. First, we notice that P2 shows significantly higher T_g, consistent with their more rigid chains. Among them, P4, i.e. the polymer synthesized from 3,3′,5,5′-tetramethylbenzidine, exhibits unusually high T_g as compared to other members of the studied family. A similar phenomenon of the T_g value increase, induced by the presence of a methyl group at the ortho position with respect to nitrogen, was also observed in the polyimides[36,37] and the polyketanils.[38,39]

Table 1. UV−vis Absorption Characteristics of the Polyazomethines

	UV−vis						
		band gap [eV]					
code	solid film [nm]	E_g[c]	E_g[e]	E_g[d]	blend with PMMA[a] [nm]	polymers in chloroform[b] [nm]	polymers with MSA in chloroform[b] [nm]
P1	422	2.41	2.55	2.50	412	419	335,384
P2	412	2.49	2.69	2.70	400	417	333,383
P3	334,380	2.61	2.90	2.93	332,384	337,387	333,383
P4	330,386	2.81	2.86		336,386	340,390	334,383
P5	414	2.53	2.67	2.70	338,408	412	383
P6	418	2.50	2.69	2.65	320,380	413	317,383

[a] Concentration 0.1% (w/w) of the polyazomethine and PMMA. [b] Concentration = 10^{-5} mol/L. [c] Band gaps were calculated from the absorption spectra of the polymer films. [d] Band gaps determined from electrochemical experiment in dichloromethane solution. [e] Band gaps were calculated from the absorption spectra of the polymer in dichloromethane solution.

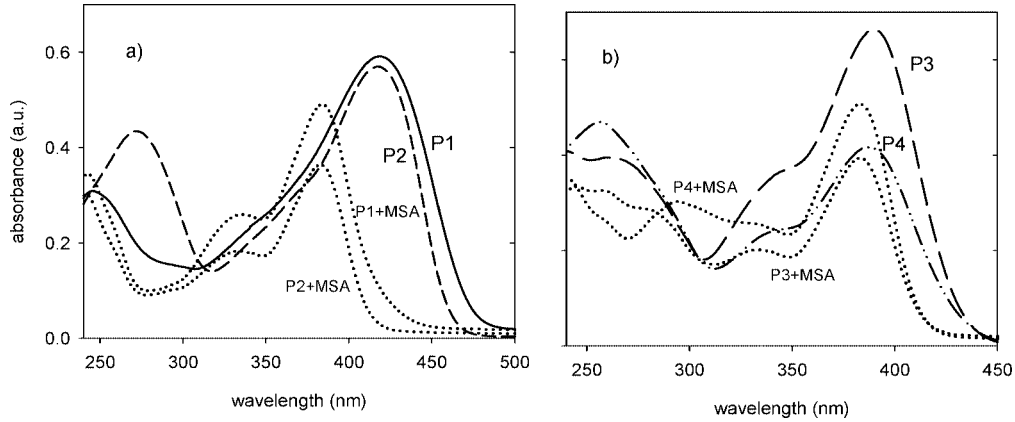

Figure 5. Chloroform solution UV−vis absorption spectra of the undoped and doped with MSA polyazomethines.

3.4. Solubility. These new polymers showed different solubility behavior in different organic solvents. Polymer solubility was qualitatively determined by the dissolution of 2.5 mg of the solid polymer in 1 mL of organic solvent at room temperature and 50 °C. The polymers P1, P4, and P5 could be easily soluble in such solvents as toluene, THF, DMA, DMF, and NMP. P2 is soluble in polar solvents, such as DMA, DMF, and NMP, while it is partially soluble in common organic solvents, such as toluene and THF. Polymer P3 is fully soluble only in NMP after heating and partially soluble in toluene, THF, and DMA. All polymers showed improved solubility compared with common polyazomethines.[20]

3.5. UV−vis Investigations. Electronic spectra of the polyazomethines were detected in chloroform solution (concentration 10^{-5} mol/L) before and after protonation with MSA, CSA, MC, CP, and PDP. Optical properties of the polyazomethines also in solid state (thin films) and in blend with PMMA were investigated. The results of the optical absorption measurements of the polyazomethines are collected in Table 1.

3.5.1. UV−vis of the Polyazomethines in Solution. The UV−vis spectra of the polyazomethines also provided additional evidence confirming their molecular structures. In the following discussion, the effects of structural modifications will be explored in terms of the effects of backbone variation. The absorption spectra of the polyazomethines in chloroform solution are characterized by one or two bands. The polymers P1, P2, P5, and P6 exhibited one well-defined absorption band in the range of 412−419 nm, being responsible for $\pi-\pi^*$ transition in the imine group (see Table 1). However, the shape of the band was not symmetrical, and a broad "tail" toward shorther wavelength was observed what suggested the overlapping with another band. An instructive example of this approach is given in Figure 5a.

Additionally, the effect of incorporation of methyl groups and more phenylene rings on the polymer backbone on the optical properties was tested. For example, the introduction of a four methyl groups as in P3 in comparison with P1 results in a hypsochromic shift of the λ_{max} band in chloroform solution from 419 to 387 nm. Simmilar behavior for the polymer P4 was observed (compare with P2). Moreover, the substituents influence also on the absorption band shape and additional band at about 336 nm was clearly visible only for the polymers P3 and P4 (see Figure 5b). This band, described as transition in triphenylamine unit, was overlapped with the band at longer wavelength in other polyazomethines. On the other hand, the introduction of a biphenyl unit between the imine groups as in P2 in comparison with P1 has no influence on absorption shift in UV−vis spectra. Similar behavior for the substituted polymers P3 and P4 was observed (see Table 1). The observed changes of the optical absorption spectra when the backbone structure is varied can be attributed to the modification of the polymer chain planarity.

3.5.2. UV−vis of the Polyazomethines in Solid State. Additionally, we have studied the absorption spectra of thin films obtained by casting chloroform solution of the polyazomethines on the glass (see Table 1). UV−vis absorption bands in the polymer thin films spectra were only a little shifted in comparison with the ones detected in chloroform solution. This seems to indicate that the chain conformations in solution can be partially maintained in the films cast from the same solvent.

The band gaps (E_g) of the polymer films were calculated from the optical absorption edge and were significantly dependent on the polymers structure (see Table 1). It is well-known that the higher value of E_g indicates the shorter conjugation units in the polymer chains, which is also manifested in a blue shift of the electronic absorption band. The difference between the E_g of the polymers P1 and P2 was only 0.08 eV, while between P3 and P1 it was 0.20 eV. The four methyl groups caused increase of E_g value in comparison with the unsubstituted analogues (see Table 1). For example, the E_g value for P4 icrerase 0.32 eV in comparison with P2.

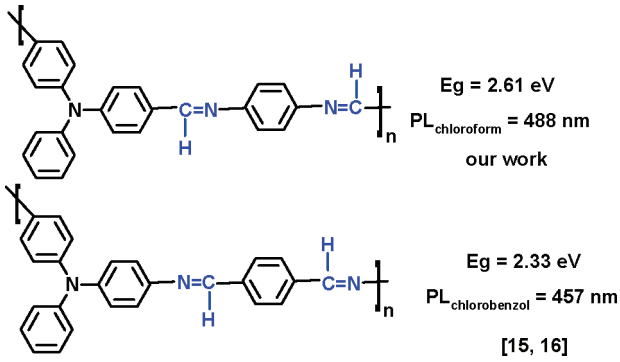

Figure 6. Chemical structure and E_g and PL of the two polyazomethines.

The differences found in energy gap values along with the maximum electronic absorption bands confirm the difference planarity of the *N*-phenylene ring toward the imine linkage and different conformations of the polymer chains and as a consequence the different length of the conjugated units.

As it was mentioned before, Niu et al.[10,11] synthesized the polyazomethine from 4,4′-diaminotriphenylamine and terephthalic aldehyde, in which the imine groups exhibited reverse position in comparison with the polymer P1 (see Figure 6).

They found the energy gap for their polymer detected in chloroform solution at 2.33 eV. In the case of P1 the energy gap in chloroform solution was found to be 2.61 eV. The difference indicates a little worse conjugation in the polymer P1 in comparison with the one studied by Niu.[10,11]

Additionally, we have studied the absorption spectra of free transparent foils obtained by casting chloroform solution of the polyazomethines with a nonemissive polymer, poly(methyl methacrylate) (PMMA) at concentration 0.1% w/w (see Table 1). In most cases the absorption bands were hypsochromically shifted in blends in comparison with the proper polymers thin films, being in the range of 6−12 nm (see Table 1). The exception was the polymer P6 with the methoxy substituents where the blue shift was equal to 38 nm. It is also worth expressing that in the absorption spectra of P5 and P6 blends additional absorption bands at shorter wavelengths at 338 and 320 nm, respectively, were seen, contrary to the proper polymer thin films spectra. However, the conformation of the polymer chains can be different in dependence on the surroundings. In Figure 7 the UV−vis spectra of P1 and P3 in solution, thin film, and blend are presented.

3.5.3. UV−vis of the Doped Polyazomethines in Solution. The lone electron pair of the nitrogen atom in the imine group can be protonated or can form H-bond with the proper compounds, and this was always expected to influence on better conjugation in the polymer chains. In our work MSA, CSA, MC, CP, and PDP were used as dopants in the mole ratio of dopant to polymer mer unit being 2:1 in chloroform solution (see Figure 2). Significant changes in the electronic spectra after adding MSA and CSA were observed for the polyazomethines P1, P2, P5, and P6, while for P3 and P4 changes were little (see Table 1). However, in all cases, addition of MSA affected a hypsochromic shift of the absorption bands in UV−vis spectra. Protonation of the polymer P1 caused 35 nm hypsochromic shift of the band responsible for $\pi-\pi^*$ transition in the imine group, while in P3 the shift was only 4 nm (see Table 1). Similar behavior was observed for the polymers P2 and P4. This indicates that the presence of the methyl groups at ortho position in *N*-phenylene ring (P3 and P4) because of steric hindrance made it difficult to change planarity of the polymer chain. Moreover, it should be noted that in the presence of MSA additional absorption bands in UV−vis spectra at about 335 nm for P1 and P2 were detected. In Figure 5 the electronic spectra of P2 and P4 before and after protonation with MSA are presented. Similar results were obtained when CSA was used as a protonating agent. When the polyazomethines under investigations were doped with phenolic type compounds (MC, CP, PDP), no changes of the electronic absorption bands were observed, independent of the dopant acidity.

3.6. Photoluminescence of the Polyazomethines. The emission wavelength of a polymer depends on the band gap between the HOMO and LUMO, and it is connected with π-electrons delocalization along the polymer backbone. This means that the polymer chain architecture, various chain conformations, and possibilities of interactions with surroundings as solvents, dopants, or blending polymers can influence the photoluminescence.

In our work emission spectra were considered from the three points of view: (i) changing the main chain molecular structure, (ii) blending a light emitting polymer with another nonemissive polymer, and (iii) doping. Maximum emission wavelengths along with full width at half-maximum (fwhm) and bands symmetry, along with the Stokes shift values, are collected in Table 2.

3.6.1. PL of the Polyazomethines in Solution. It is know that optical properties of polymers can be tuned by chain engineering. For example, in chloroform solution P1 emitted light at longer wavelength than the P2; the difference was equal to 11 nm. The introduction of a methyl groups, i.e. the transformation of P1 into P3, results in a hypsochromic shift of the PL band from 488 to 466 nm (see Table 2 and Figure 8). Simmilar behavior for the polymer P2 in comparison with P4 was observed (see Table 2). We not observed changes in maximum of emission band for the polymers P5 and P6 in comparison with P2. However, two methyl substituents at the ortho position in the diamines (P5, P6) had an influence on the full width at half-maximum (fwhm) of the band and the band symmetry. The bands were wider and more symmetrical as indicated the values of *a*/*b*, being a relation of the part of the width at short-wavelength side (*a* in Table 2) and long-wave side (*b* in Table 2).

On the other hand, the effect of incorporation of more methyl groups on the polymer backbone on the photoluminescence properties was tested. For example, the introduction of a four methyl groups as in P4 in comparison with P5 results in a hypsochromic shift of the maximum of emission band in chloroform solution from 477 to 462 nm (see Table 2).

Even though the schematic structures of the polyazomethines seem similar, it is necessary to point out that the interchain distance depends on the diamine subunit in the polyazomethine chain.

Relative photoluminescence intensity of the polymers investigated in chloroform solution was found about 0.30% as compared with the chloroform solution emission of 9,10-diphenylanthracene used as a standard.

3.6.2. PL of the Polyazomethines in Solid State. Additionally, we have studied the emission spectra of free transparent foils obtained by casting chloroform solution of the polyazomethines with a nonemissive polymer, PMMA, at concentration of about 0.1% (see Table 2). PL spectra of the polyazomethines blends differed little in comparison with the ones detected in chloroform solution (see Figure 9).

The values of fwhm of the spectra detected in blends were smaller than the ones in chloroform solution. This indicates the more limited distribution of the polymers conformers in the blends.[40] In the case of the unsubstituted polymers P1 and P2 in blends the bands were more symmetrical (values *a*/*b* are closer to 1), contrary to the substituted P3 and P4, exhibiting

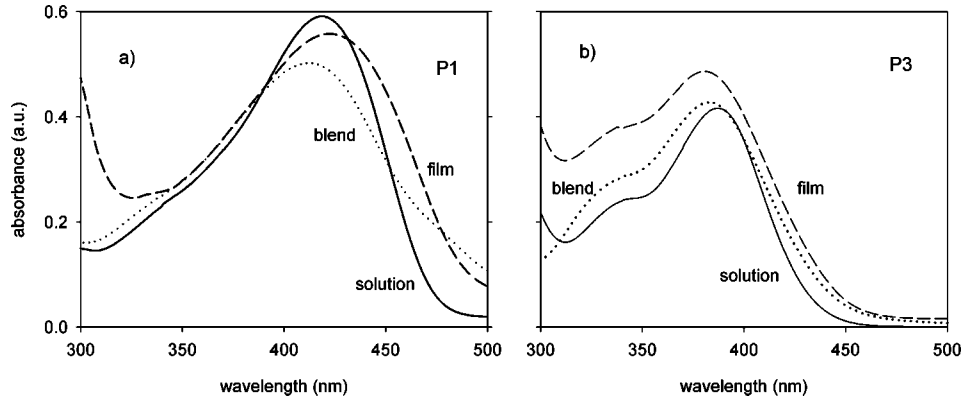

Figure 7. UV−vis spectra of P1 (a) and P3 (b) in solution, solid film, and polymer blend.

Table 2. Photoluminescence Properties of the Polyazomethines

	photoluminescence, exc = 400 nm												
	in blend with PMMA				in chloroform ($c = 10^{-4}$ mol/L)								
	0.1% w/w				pristine				MSA doped				
code	λ_{emis} [nm]	fwhm [nm]	*a*/*b*	Stokes shift[a] [cm^{-1}]	λ_{emis} [nm]	fwhm [nm]	*a*/*b*	Stokes shift [a] [cm^{-1}]	λ_{emis} [nm]	fwhm [nm]	*a*/*b*	Stokes shift[a] [cm^{-1}]	$\Delta\lambda_{emis}$[b] [nm]
P1	482	43	0.59	3525	488	45	0.50	3380	465	58	0.66	4537	−23
P2	470	49	0.63	3723	477	43	0.48	3017	460	65	0.62	4371	−17
P3	490	50	0.56	5634	466	57	0.73	4381	461	63	0.66	4418	−5
P4	460	51	0.58	4303	462	53	0.77	3996	462	63	0.80	4465	0
P5	nm	nm	nm	nm	477	42	0.45	3308	460	62	0.63	4371	−17
P6	nm	nm	nm	nm	480	42	0.55	3380	460	59	0.64	4371	−20

[a] Calculated according to the equation $\nu_{abs} - \nu_{emis} = (1/\lambda_{abs} - 1/\lambda_{emis}) \times 10^7$ [cm^{-1}]. [b] Shift of undoped and doped polyazomethines in chloroform solution; "−" means blue shift.

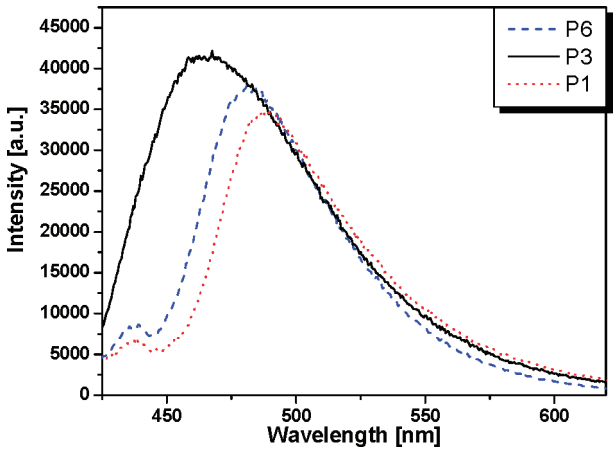

Figure 8. PL spectra of 1×10^{-4} mol/L polymers in chloroform solution under 400 nm excitation wavelength.

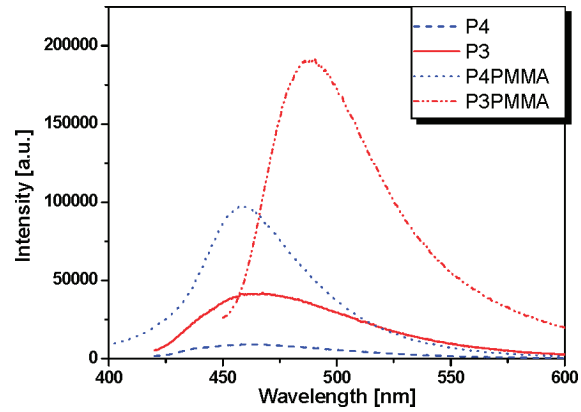

Figure 9. PL spectra of the polyazomethines P3 and P4 in chloroform solution and the polyazomethines/PMMA polymer blends under 400 nm excitation wavelength.

the values *a*/*b* being smaller than the ones detected in chloroform.

Stokes shift of the absorption and emission wavelengths is an important parameter which indicates the differences in properties and structures of the polymers. The calculated Stokes shift values for P1, P2, P3, and P4 in chloroform solution indicated significant differences in the energy loss, which occurred during transition from S_0 to S_1. The higher values were observed for the polymers P3 and P4 (see Table 2). On the other hand, the polymers P5 and P6 exhibited Stokes shift values close to that of the unsubstituted polyazomethine P2. The Stokes shift values were found to be higher for the proper polyazomethines in blend in comparison with the ones in chloroform solution, which illustrates that more energy loss occurred during the transition from S_0 to S_1 in the solid state.

3.6.3. PL of the Doped Polyazomethines in Solution. PL spectra of the doped with MSA polyazomethines under 400 nm excitation wavelength have a broad emission band at 460−465 nm, which are blue-shifted from the corresponding undoped polymers (see Table 2). The biggest shift after protonation for the polymers P1 and P2 was observed, being equal to 23 and 17 nm, respectively. Hypsochromic shift of the emission wavelength indicated the shorter conjugation units in the polymer chain.[40]

The progressive blue shifts of the PL spectra of the polyazomethines are accompanied by significant broadening of the emission band after dopping with MSA (see Figure 10a) which seems to indicate higher conformational disorder of the polymers chains. On the other hand, the emission bands of the polymers after protonation were more symmetrical, which was the result of increasing of the part of fwhm width at short-wavelength side (a).

The full width at half-maximum (fwhm) of the emission spectrum of the undoped and doped polyazomethines increases

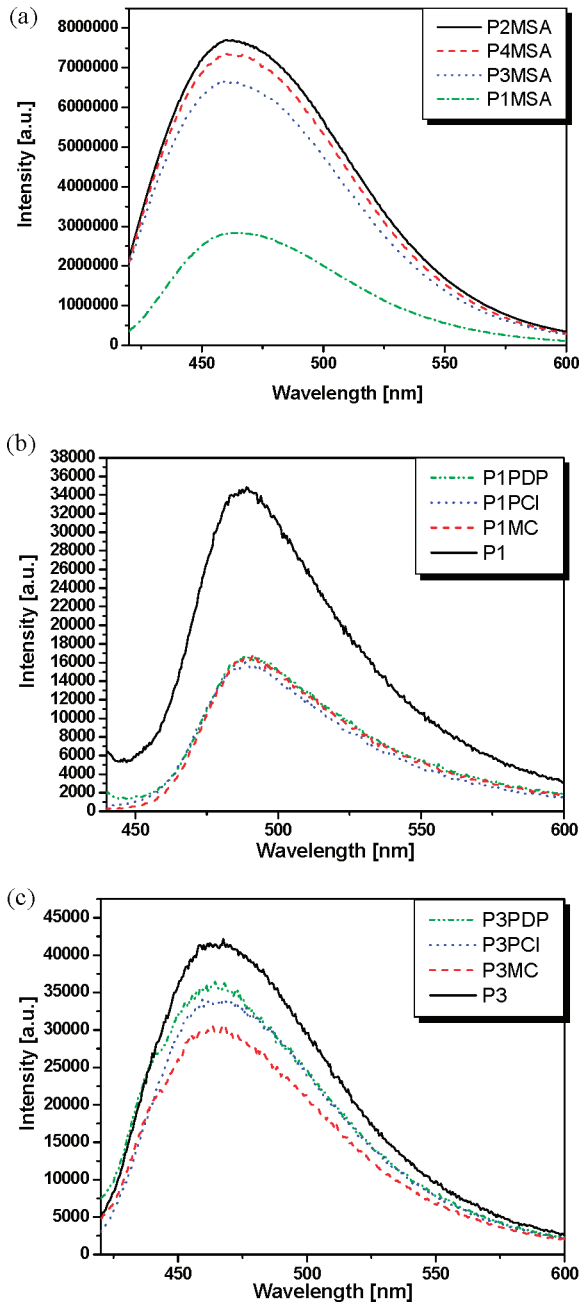

Figure 10. PL spectra of the doped with MSA polyazomethines (a), undoped and doped with phenols P1 (b), and undoped and doped with phenols P3 (c) in chloroform solution under 400 nm excitation.

from 42−57 to 58−63 nm in chloroform solution (see Table 2). The smallest increase of fwhm for the doped polymer P3 in comparison with the undoped one was found (see Table 2).

The values of the energy loss increased in all the polyazomethines after protonation, even though the differences between pristine and protonated polymers were much higher in the P1 (1157 cm^{-1}) and P2 (1354 cm^{-1}) than in the substituted P3 (37 cm^{-1}) and P4 (469 cm^{-1}).

It should be also noted that the protonation influences not only the emission wavelength but also the intensity of the photoluminescence.[41] Figure 10a presents the photoluminescence intensity in cps of the polyazomethines studied in their protonated form.

First we notice that the luminescence intensity in conjugated systems is very sensitive with respect to the imine sites protonation. In all cases it is improved by a factor 2.00. The relative PL intensity of the doped with MSA polymers investigated in chloroform solution was found about 20% as compared with the chloroform solution emission of 9,10-diphenylanthracene used as a standard. It is therefore clear that the protonation not only lowers the luminescent excited state but also influences the electronic structure of the fully conjugated backbone in such a manner that the probability of the radiative transition is increased.

Table 3. Electrochemical Potentials and Energy Levels of the Polymers P1 and P3

code	E_g (eV)[c]	E_{pa} (eV)	E_{pc} (eV)	$E_{1/2}$ (eV)	HOMO[a] (eV)	LUMO[b] (eV)
P1	2.50	−1.5	−1.14	−1.32	−5.78	−3.28
P3	2.93	−1.7	−1.25	−1.47	−5.93	−3.00

[a] HOMO levels were converted from measured oxidation potentials assuming the absolute energy level of Fc to be −4.8 eV. [b] LUMO levels were estimated from the HOMO levels and energy gaps. [c] Band gaps were calculated from electrochemical experiment in dichloromethane solution.

Even though the schematic structures of the protonated polyazomethines seem similar, it is necessary to point out that the distances between the cations located on nitrogen atoms are different which causes the MSA anions to have different special distances. This fact may influence the different geometries of the macromolecules. When Bronsted acids are used as protonating agent, changes in the properties are due to molecular recognition and formation of supramolecular structures of the polymers chains based on hydrogen or ionic bonding between an acidic type dopant and basic center in the polymer chain. In this case conformational changes induced by polymer−dopant interactions alter the π-orbital overlap in the polymer chain, which results in the energetic change in the electronic transitions. However, efficiency of the acid−base doping may depend not only on the dopant acidity but also on its steric structure and accesibility to the basic center which depends on the polymer chain conformation and the presence of bulky substituents. Another important class of molecular interactions is hydrogen bonding, which is particularly useful in constructing molecular assemblies. However, in our case no shifts of the emission wavelengths were observed in the presence of the phenolic type dopants (see Figure 10b,c).

3.7. Cyclic Voltammetry. The energy levels of the polymers were calculated using ferrocene (Fc) value of −4.8 eV as the standard ($E_{Fc} = E_{Ag} - 0.089$ V). The HOMO (highest occupied molecular orbital) levels of materials were obtained as $E_{1/2}$ that were calculated as the average between E_{pa} (anodic peak) and E_{pc} (cathodic peak). The values of E_{pa} and E_{pc} correspond to maximum and minimum peak of oxidation potential curve, respectively. The LUMO (lowest occupied molecular orbital) levels are estimated as deduction band gap calculated from UV edge from HOMO values. All the electronic parameters from CV are summarized for P1 and P3, as an example in Table 3. In our work CV in dichloromethane was made, opening a possibility for solution electrochemical studies.

Figure 11a shows cyclic voltammetry curves for P1 and P3, as an example. Oxidation of each polymer is a two-step process with the first step taking place at ca. 1.5 V and the second one at 1.7 V. The course of the reduction half-cycle indicates that this process is reversible, yet only the first redox step is characterized by a well-defined peak taking place at 1.14 V for P1 and 1.25 V for the P3.

Protonation of the investigated polymers is also feasible; however, no clear reduction peak could be recorded as the reduction process of these polymers takes place near the basic electrolyte's working potential window boundary. Signature of this process, though, is clearly visible on the DPV curve shown in Figure 11b. As a result, the peak's onset potential can be determined being equal to −1.60 and −1.75 V for the polymers P1 and P3, respectively. Consequently, this enabled us to determine the polymers' band gaps electrochemically.

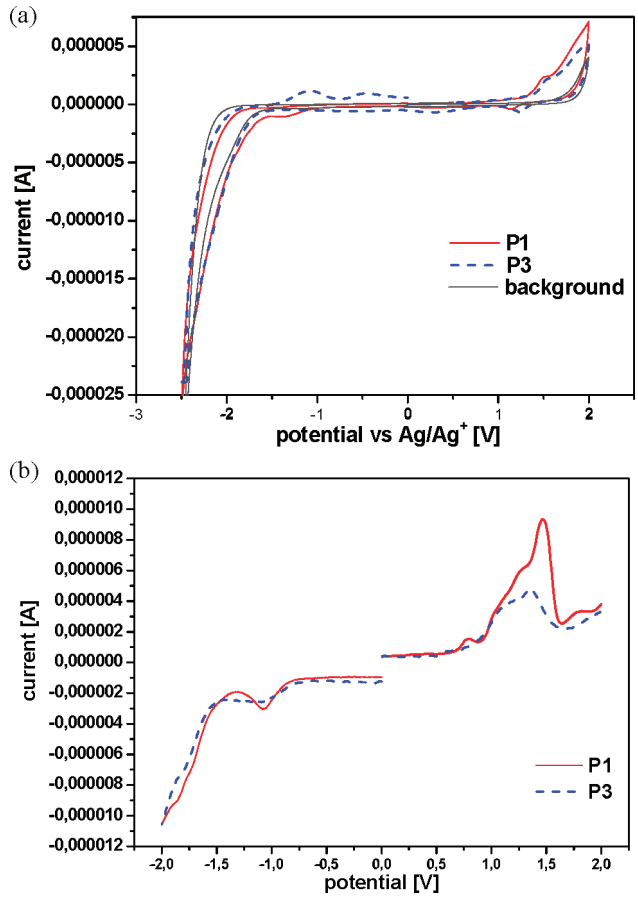

Figure 11. Cyclic voltammetry (a) and differential pulse voltammetry plots of the polymers P1 (solid line) and P3 (dashed line) and background (thin gray line). Sweep rate 100 mV/s.

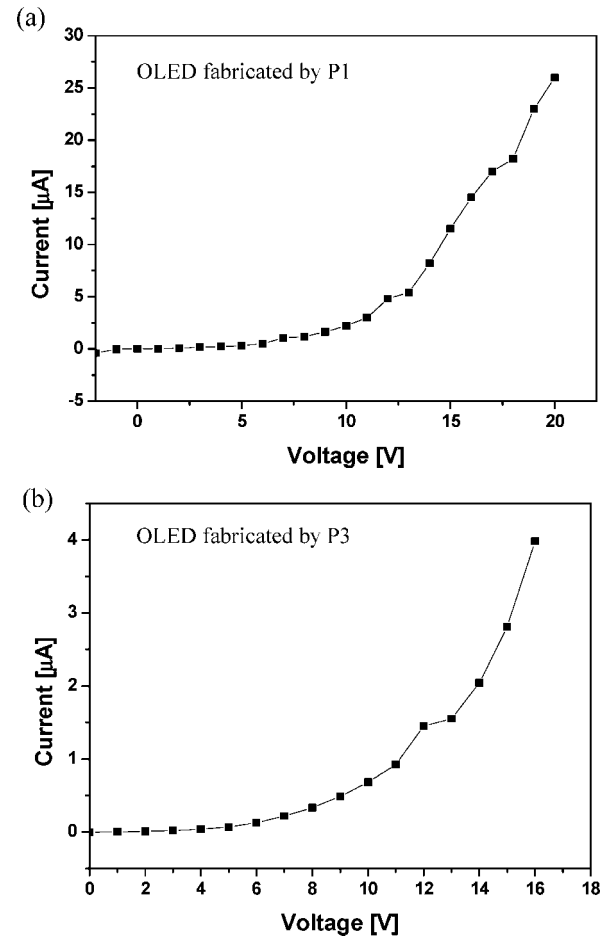

Figure 12. Current−voltage curves of ITO/P1/Alq_3/Al (a) and ITO/P3/Alq_3/Al (b) devices.

With the exception of P4, for which the reduction process could not be observed in the available potential range, the results of both methods agree well. Detailed electrochemical and spectroelectrochemical studies are currently in progress.

3.8. Current−voltage Characteristics. Current−voltage curves of ITO/P1/Alq_3/Al and ITO/P3/Alq_3/Al are shown in Figure 12. It can be seen that current increases with applied voltage increase, which confirms the semiconducting properties of the polyazomethine films. The turn-on voltage of the devices was observed at about 6 V in room temperature, and no significant differences between P1 and P3 were seen. Further investigations are in progress.

4. Conclusions

A series of new aromatic polyazomethines with triphenylamine core in the main chain has been synthesized by high-temperature solution polycondensation. The resulting polymers were soluble in organic solvents and formed transparent films on glass. The polyazomethines emitted blue or blue-green light. Absorption and emission spectroscopies along with cyclic voltametry have shown a significant influence of the diamines structures on the properties of these conjugated polyazomethines. The effect of protonating agent—MSA or CSA—on the optical properties was investigated.

The following conclusions can be drawn from the present work:

1. The photoluminescence properties in chloroform solution under 400 nm excitation wavelength exhibit all polyazomethines and are observed in the range of 462−488 nm, depending on the diamine subunit. PL spectra of the polyazomethines blends with PMMA differed little in comparison with the ones detected in chloroform solution.

2. Relative photoluminescence intensity of the polymers investigated in chloroform solution was found about 0.30% as compared with the chloroform solution emission of 9,10-diphenylanthracene used as a standard.

3. MSA, in association with the polyazomethines, modifies the electronic properties of these compounds and by consequence alters their absorption and photoluminescence as an effect of the imine sites protonation. PL spectra of the doped with MSA polyazomethines under 400 nm excitation wavelength have a broad emission band at 460−465 nm, which are blue-shifted from the corresponding undoped polymers.

4. The relative PL intensity of the doped with MSA polymers investigated in chloroform solution was found about 20% as compared with the chloroform solution emission of 9,10-diphenylanthracene used as a standard.

5. The band gaps (E_g) of the polymer films were calculated from the optical absorption edge and were observed at the range 2.41−2.81 eV depended on the polymers structure.

6. HOMO−LUMO levels of the polyazomethines by cyclic voltametry in solution were detected. In solution LUMO of the polyazomethines P1 and P3 can be estimated as −3.28 and −3.00 eV, respectively, while HOMO of the polymers P1 and P3 in solution can be estimated as −5.78 and −5.93 eV, respectively.

7. Preliminary investigations of the current−voltage characteristics for device such as ITO/P1/Alq_3/Al and ITO/P3/Alq_3/Al confirmed their semiconductivity properties of the organic thin film.

Acknowledgment. This work was financially supported in the frame of expenditure on science (2006−2007) (Grant 1T09B 088 30). The authors thank the Department of Earth Sciences, Silesian University in Sosnowiec, for making it possible to do the fluorescence spectra measurements. The authors also thank Dr. H. Janeczek for DSC measurements.

References and Notes

(1) Friend, R. H.; Gymer, R. W.; Holmes, A. B.; Burroughes, J. H.; Marks, R. N.; Taliani, C.; Bradley, D. D. C.; Dos Santos, D. A.; BréDas, J. L.; LöGdlund, M.; Salaneck, W. R. *Nature (London)* **1999**, *397*, 121–128.
(2) Kim, D. Y.; Cho, H. N.; Kim, C. Y. *Prog. Polym. Sci.* **2000**, *25*, 1087–1139.
(3) Tabata, M.; Fukushima, T.; Sadahiro, Y. *Macromolecules* **2004**, *37*, 4342–4350.
(4) Sanda, F.; Nakai, T.; Kobayashi, N.; Masuda, T. *Macromolecules* **2004**, *37*, 2703–2708.
(5) Tang, B. Z.; Chen, H. Z.; Xu, R. S.; Lam, J. W. Y.; Cheuk, K. K. L.; Wong, H. N. C.; Wang, M. *Chem. Mater.* **2000**, *12*, 213–221.
(6) Qu, J.; Kawasaki, R.; Shiotsuki, M.; Sanda, F.; Maruda, T. *Polymer* **2006**, *47*, 6551–6559.
(7) Kim, D. U.; Kim, S. H.; Tsutsui, T. *Synth. Met.* **2001**, *123*, 43–46.
(8) Ma, C. Q.; Zhang, B. X.; Liang, Z.; Xie, P. H.; Wang, X. S.; Zhang, B. W. *J. Mater. Chem.* **2002**, *12*, 1671–1675.
(9) Thomas, K. R. J.; Lin, J. T.; Tao, Y. T.; Chuen, C. H. *Adv. Mater.* **2002**, *14*, 822–826.
(10) Niu, H.; Huang, Y.; Bai, X.; Li, X.; Zhang, G. *Mater. Chem. Phys.* **2004**, *86*, 33>37.
(11) Niu, H.-J.; Huang, Y.-D.; Bai, X.-D.; Li, X. *Mater. Lett.* **2004**, *58*, 2979–2983.
(12) Meng, F.; Liu, Ch.; Hua, J.; Cao, Y.; Chen, K.; Tian, H. *Eur. Polym. J.* **2003**, *39*, 1325>1331.
(13) Hua, J. L.; Li, B.; Meng, F. S.; Ding, F.; Qian, S. X.; Tian, H. *Polymer* **2004**, *45*, 7143–7149.
(14) Meng, F.; Mi, J.; Qian, S.; Chen, K.; Tian, H. *Polymer* **2003**, *44*, 6851–6855.
(15) He, Q.; Huang, H.; Lin, H.; Yang, J.; Bai, F. *Synth. Met.* **2003**, *135−136*, 165–166.
(16) Bernius, M. T.; Inbasekaran, M.; O'Brien, J.; Wu, W. S. *Adv. Mater.* **2000**, *12*, 1737–1750.
(17) Stolka, M.; Yanus, J. F.; Pai, D. M. *J. Phys. Chem.* **1984**, *88*, 4707–4714.
(18) Thelakkat, R.; Fink, R.; Haubner, F.; Schmidt, H. W. *Macromol. Symp.* **1997**, *125*, 157.
(19) Thelakkat, M. *Macromol. Mater. Eng.* **2002**, *287*, 442–461.
(20) Iwan, A.; Sek, D. *Prog. Polym. Sci.* **2008**, *33*, 289–345.
(21) Adams, R.; Bullock, R. E.; Wilson, W. C. *J. Am. Chem. Soc.* **1923**, *45*, 521–527.
(22) Marvel, C. S.; Hill, H. W. *J. Am. Chem. Soc.* **1950**, *72*, 4819–4820.
(23) Marvel, C. S.; Bonsignone, P. W. *J. Am. Chem. Soc.* **1959**, *81*, 2668–2670.
(24) D'Alelio, G. F.; Crivello, J. V.; Schoening, R. K.; Huemmer, T. F. *J. Macromol. Sci.* **1967**, *A1*, 1161–1249.
(25) Reinhardt, B. A.; Unroe, M. R. *Polym. Commun.* **1991**, *32*, 85–87.
(26) Bryant, R. G. *Polym. Prepr.* **1992**, *33*, 182–183.
(27) Kim, D. U.; Kim, S. H.; Tsutsui, T. *Synth. Met.* **2001**, *123*, 43–46.
(28) Ma, C. Q.; Zhang, B. X.; Liang, Z.; Xie, P. H.; Wang, X. S.; Zhang, B. W. *J. Mater. Chem.* **2002**, *12*, 1671–1675.
(29) Thomas, K. R. J.; Lin, J. T.; Tao, Y. T.; Chuen, C. H. *Adv. Mater.* **2002**, *14*, 822–826.
(30) Ikkala, O.; ten Brinke, G. *Science* **2002**, *295*, 2407–2409.
(31) Yang, C. J.; Jenekhe, S. A. *Macromolecules* **1995**, *28*, 1180–1196.
(32) Jung, S. H.; Lee, T. W.; Kim, Y. C.; Suh, D. H.; Cho, H. N. *Opt. Mater.* **2002**, *21*, 169–173.
(33) Siling, S. A.; Lozinskaya, E. I.; Borissevitch, Yu. E. In *Recent Advances in Polymer Chemical Physics*; Contributions of the Russian Academy of Sciences; Prevorsek, D. C., Ed.; Gordon and Breach Science Publishers, CRC Press: Boca Raton, FL, 1998; Chapter 9, p 239.
(34) Silling, S. A.; Lozinskaya, E. I.; Boressevitch, Yu. E. *Oxid. Commun.* **1997**, *20*, 149–168.
(35) Meng, F.; Liu, Ch.; Hua, J.; Cao, Y.; Chen, K.; Tian, H. *Eur. Polym. J.* **2003**, *39*, 1325–1331.
(36) Eastmond, G. C.; Paprotny, J.; Webster, I. *Polymer* **1993**, *34*, 2865–2874.
(37) Eastmond, G. C.; Page, P. C. B.; Paprotny, J.; Richards, R. E.; Shaunak, R. *Polymer* **1994**, *35*, 4215–4227.
(38) Iwan, A.; Sek, D.; Rannou, P.; Kasperczyk, J.; Janeczek, H.; Mazurak, Z.; Proń, A. *Synth. Met.* **2004**, *143*, 331–339.
(39) Iwan, A.; Sęk, D.; Kasperczyk, J. *Macromolecules* **2005**, *38*, 4384–4392.
(40) Yang, C. Y.; Hide, F.; Diaz-Garcia, M. A.; Heeger, A. J.; Cao, Y. *Polymer* **2004**, *39*, 2299–2304.
(41) Knaapila, M.; Ikkala, O.; Torkkeli, M.; Jokela, K.; Serimaa, R.; Dolbnya, I. P.; Bras, W.; Horsburgh, L. E.; Palson, L. O.; Monkman, A. P. *Appl. Phys. Lett.* **2002**, *81*, 1489–1491.

MA702637K